J. Fish. Sci. Tech. 5(3), 219~228, 2002

JOURNAL OF
FISHERIES SCIENCE
AND TECHNOLOGY

Eddy Kinetic Energy in the East Sea Estimated from Topex/Poseidon Altimeter Measurements

Kwangwoo Cho[+] and Kyu-Dae Cho[1]

Environmental Impact Assessment Division, Korea Environment Institute, Seoul, Korea
[1]Department Of Oceanography, Pukyong National University, Busan 608-737, Korea

(Received January 2002, Accepted September 2002)

Based on the five-year (October 1992 through September 1997) Topex/Poseidon altimeter measurements, we describe the statistical characteristics of the eddy variability in the East Sea in terms of sea surface height anomaly, slope variability, and eddy kinetic energy (EKE). The sea surface height anomalies in the East Sea are produced with standard corrections from Topex/Poseidon measurements. In order to eliminate the high frequency noise in the sea surface height anomaly data, the alongtrack height anomaly data was filtered by about 40 km low-pass Lanczos filter based on Strub et al. (1997) and Kelly et al. (1998). We find that there exists a distinct spatial contrast of high eddy variability in the south and low eddy energy in the north, bordering the Polar Front. In the northwestern area (north of 39°N and west of 133°E) from the Polar Front where the eddies frequently appear, the EKE is also considerable. The high kinetic energy in the southern East Sea reveals a close connection with the paths of the Tsushima Warm Current, suggesting that the high variability in the south is mainly generated by the baroclinic instability process of the Tsushima Warm Current. This finding is supported by other studies (Fu and Zlontnicki, 1989; Stammer, 1997) which have shown the strong eddy energy coupled in the major current system. The monthly variation of the EKE in both areas of high and low eddy variability shows a strong seasonality of a high eddy kinetic energy from October to February and a relatively low one from March to September. The sequential pattern of wind stress curl shows resemblance with those of monthly and seasonal EKE and the two sequences have a correlation of 0.82 and 0.67, respectively, providing an evidence that wind stress curl can be the possible forcing for the monthly and seasonal variation of the EKE in the East Sea. The seasonality of the EKE also seems to correlate with the seasonality of the Tsushima Warm Current. There also exists the large spatial and interannual variabilities in the EKE.

Key words: Eddy kinetic energy, Mesoscale eddy, Oceanic variability, Altimeter application, East Sea

Introduction

The Topex/Poseidon spacecraft, jointly conducted by the National Aeronautics and Space Administration (NASA), USA and Centre National d'Etudes Spatiales (CNES), France, measures the altitude between the spacecraft and sea surface with a radar altimeter deployed in an orbit specially designed for precise measurements. The Topex/Poseidon is the first altimeter mission designed for ocean circulation and its variability by observing the sea surface topography from space (Fu et al., 1994). The spacecraft provides the altitude observations with global coverage every 9.91 days and with a horizontal alongtrack resolution of about 6.2 km. The altitude is converted into sea surface topography (and thus surface geostrophic current) with a variety of corrections and geoid information. The corrections include instrument, atmospheric refraction, air-sea interaction, and external geophysical corrections (Chelton, 1988). The altimeter data of the previous missions such as Seasat and Geosat had a lot of errors

[+]Corresponding author: kwcho@kei.re.kr

including large orbit error. The accuracy and precision of the Topex/Poseidon instrument are now at a level of 5~10 cm and 1 cm, respectively (Stammer and Wunsch, 1994). The altimeter data acquired by the Topex/Poseidon have been applied in the broad field of ocean dynamics including the eddy variability of ocean in different oceans of the world.

Though oceanic variability has a variety of spatial and temporal scales, mesoscale eddies with a spatial scale of 40~500 km and temporal scale of 20~50 days are dominant in the ocean and the dominance has been observed by the ship drift measurements (Wyrtki et al., 1976), drifting buoys (Richardson, 1983), and altimeter measurements (Wunsch and Stammer, 1995). The understanding of energetic mesoscale eddy in the ocean is very important because eddies in the ocean transport momentum, heat, and passive tracers (for example, plankton and larvae), and also interacts with mean flow and climate. The theoretical studies suggest that the mesoscale eddy of ocean be mainly generated by instability processes (McWilliams, 1983; Robinson, 1983), variable wind forcing (Muller and Frankignoul, 1981), and topography (Treguier and Hua, 1988). Previous studies on the eddy variability using altimeter data are abundant throughout the world oceans (Zlontnicki et al., 1989; Fu and Davidson, 1995; Stammer, 1997; Kelly et al., 1998; Jacobs et al., 1999). In the global application of the Topex/Poseidon data, Stammer (1997) characterized the eddy variability over the world ocean. He found that the strong eddy variability was shown in the major ocean current system and hypothesized that the major eddy-generation mechanism is baroclinic instability, not only near major current but on a broad basis. Zlontnicki et al. (1989) found that the sea level variance in the northeastern Pacific Ocean and northeastern Atlantic Ocean is higher in both the fall and winter than the yearly averages based on the Geosat altimeter data, and suggested the seasonality of the sea level variance over the Oceans is induced by wind-forcing. The significant correlation between wind and sea level variability was also found in the eastern North and South Pacific Oceans (Fu and Davidson, 1995).

A variety of observations has revealed that mesoscale eddies are abundant over the East Sea (Toba et al., 1984; Isoda and Saitoh, 1993; Isoda, 1994; Lie et al., 1995; Shin et al., 1995; Jacobs et al., 1999). Toba et al. (1984) found that the synoptic circulation in the East Sea is dominated by mesoscale eddies such that the mean flow like Tsushima Warm Current is discernible only after averaging the instantaneous flow field over long period of time. Based on the satellite infrared images and hydrographic data, Isoda and Saitoh (1993) investigated the propagation of individual eddies and found that a weak meander of a thermal front was first initiated from the Korea Strait near the Korean coast, grew into an isolated warm eddy, and moved northward from spring to summer. Jacobs et al. (1999) calculated the Reynolds stress at the crossover points of Geosat and Topex/Poseidon altimeters over the East Sea. They found that the mesoscale eddies enhance the transport of the Polar Front and the separation of the East Korean Warm Current.

However, the variability study is quite limited in the East Sea, especially using a synoptic dataset such as altimeter data. The present paper is directed at investigating the spatial and temporal eddy variabilities in the East Sea from the Topex/Poseidon measurements with the aim of a quantitative description of the near surface eddy variability and clarification of possible forcing of the eddy variability. Section 2 briefly describes the Topex/Poseidon altimeter data, data processing, and analysis method for eddy variability. The spatial and temporal eddy variability in the East Sea is given and discussed in section 3 through record-length mean distribution, monthly and seasonal mean variations of eddy variability. We conclude with a brief summary and concluding remarks in section 4.

Data and Method

The Topex/Poseidon satellite altimeter data used in the present study are GDR-M products and are obtained from the Centre National d'Etudes Spatiales (CNES), France and PO.DAAC, Jet Propulsion Laboratory (JPL), USA. The record length of the data is 5 years covering the period from October 1992 through September 1997. The NASA JGM3 orbit is used for the Topex/Poseidon altitude (distance from satellite to reference ellipsoid). The geophysical corrections including dry and wet tropos-

phere corrections, ionosphere correction, and inverse barometric effect are first applied to the altitude. The dry troposphere correction and inverse barometer effect are calculated from ECMWF data, wet troposphere correction from TMR radiometer, and ionosphere correction from the dual-frequency altimeter range measurements of the Topex/Poseidon (AVISO, 1997). The sea state bias is calculated with BM4 formula (Gasper and Ogor, 1996). The components of ocean and loading tides are calculated from CSR3.0 model (Eanes and Bettadpur, 1995) and solid earth tide from a model of Cartwright and Tayler (1971). The sea surface height is then derived by subtracting the altimeter range and various corrections above from the Topex/Poseidon orbit. This process leads to corrected sea surface height. The corrected sea level height data are resampled every 7 km using cubic spline for a given track and for each cycle. The three-year mean (from January 1993~December 1995) of the corrected sea surface height data are subtracted from the corrected sea surface height data. The resulting data represent ocean variability signal relative to the three-year mean and are referred to the sea surface height anomaly data. The detailed information of the Topex/Poseidon altimeter data process can be found in Chelton (1988), AVISO (1997), and PO.DAAC (1997). Figure 1 shows the Topex/Poseidon tracks in the East Sea and the number of the data with 7 km alongtrack sampling resolution is over 1,000 points.

The eddy variability in the East Sea is investigated in terms of sea surface height anomaly, slope variability and eddy kinetic energy. The sea surface height anomaly is represented with rms (root-mean-square) value at the observation points along the track. The surface eddy kinetic energy is calculated along the satellite track from the sea surface height anomaly assuming a geostrophic relation and isotropic condition of mesoscale eddy as

$$EKE = v^2,\quad v = -\frac{g}{f}\frac{\Delta\zeta}{\Delta h}$$

where EKE is surface eddy kinetic energy, v surface geostrophic velocity component normal to the satellite track, g gravitational acceleration, f Coriolis parameter ($2\Omega\sin\theta$), ζ and h sea surface height anomaly and distance along a satellite track, respectively. The slope variability is calculated as $EKE\sin^2\theta$ to reduce the latitudinal dependency of EKE. The geostrophic velocity calculation from alongtrack altimeter data is a kind of high-pass filter process and the resulting velocity can be contaminated by high-frequency noise. However the low-pass filter with large cut-off frequency tends to filter out the signal of mesoscale eddies. Concerning optimal separation distance for the geostrophic calculation from the Topex/Poseidon data, Strub et al. (1997) found that an optimal separation scale was 40~50 km by comparing SSH derivative from the Topex/Poseidon data with observation data. Kelly et al. (1998) also compared the correlation between geostrophic velocity from the Topex/Poseidon data and drifter velocities for the choice of optimal separation distance in the calculation of geostrophic velocity from the Topex/Poseidon data. They obtained that the maximum correlation was found in a separation distance

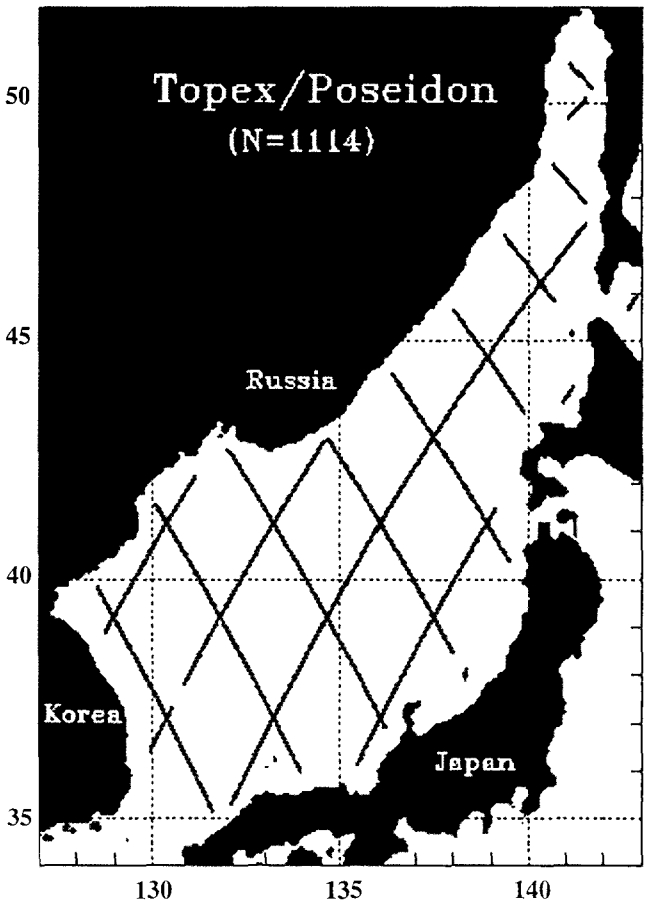

Fig. 1. Topex/Poseidon satellite subtracks in the East Sea.

of about 40 km. Based on these results (Strub et al., 1997; Kelly et al., 1998), a Lanczos low-pass filter with a half-amplitude distance of about 40 km is applied to remove the high frequency noise in the anomaly data prior to the calculation of the slope variability and eddy kinetic energy. The monthly and seasonal means, and standard deviations of the Topex/Poseidon time series at each observation point are com-puted. Any value of the time series more than three standard deviations away from mean is deleted to reduce the adverse effects of end data, outlier points, and so on.

Results and Discussion

The five-year mean distributions of the sea surface height anomaly (SSHA) and surface eddy kinetic energy (EKE) in the East Sea are shown in Figures 2 and 3, respectively. The five-point mean values of SSHA and EKE are computed and plotted along the tracks as in Fig. 1. For the visual convenience, the SSHA and EKE distributions are arbitrarily divided into three groups of low eddy variability area as small dots (SSHA<8.5 cm in Fig. 2 and EKE <150 cm^2/s^2 in Fig. 3), medium eddy variability area as medium dots (8.5 cm≤SSHA<11.5 cm and 150 cm^2/s^2≤EKE<250 cm^2/s^2), and high eddy variability area as open circles (SSHA≥11.5 cm and EKE≥250 cm^2/s^2), respectively. The figures 2 and 3 serve as a further check on the consistency between the distributions of the eddy variability in the East Sea

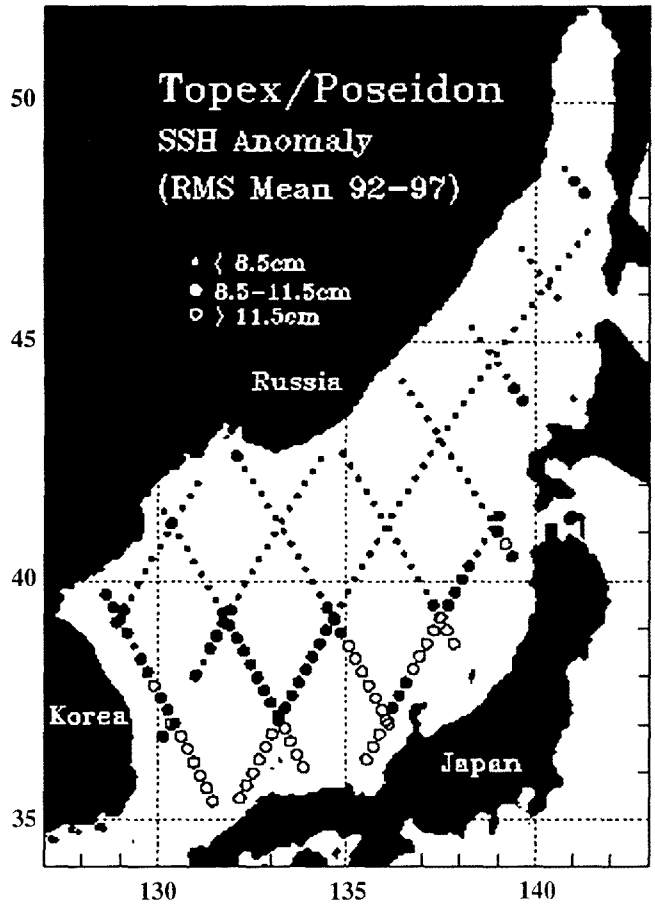

Fig. 2. RMS (Root Mean Square) sea surface height anomaly (SSHA) in the East Sea averaged for five-year (October 92~September 97) Topex/Poseidon altimeter data. Small dots represent SSHA <8.5 cm, medium dots 8.5 cm≤SSHA<11.5 cm, and open circles SSHA≥11.5.

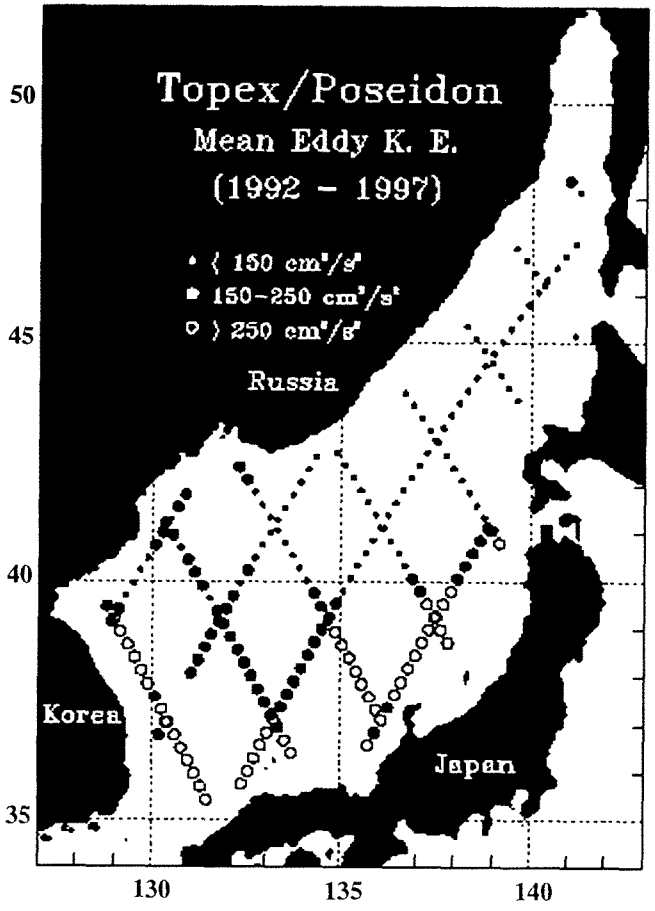

Fig. 3. Eddy kinetic energy (EKE) in the East Sea averaged for the five-year (October 92~September 97) Topex/Poseidon altimeter data. Small dots represent EKE< 150 cm^2/s^2, medium dots 150 cm^2/s^2≤EKE <250 cm^2/s^2 and open circles ≥EKE250 cm^2/s^2.

based on SSHA and EKE. The distinct spatial characteristic of the eddy variability in the East Sea is a contrast between high eddy area in the south and weak eddy area in the north with a transition between them. The strong mesoscale eddy variabilities are seen along the paths of the Tsushima Warm Current, suggesting that the baroclinic instability caused by the Tsushima Warm Current is a dominant source of the mesoscale eddy variability in the south of the East Sea. The relatively considerable amount of eddy energy is also shown in the area north of 39°N and west of 133°E (Fig. 3), where the eddy appears frequently. The meridional dependence of the background eddy variability in the East Sea can be also seen in the zonal averages of EKE and slope variability (Fig. 4). In terms of zonal averages, the high eddy variability is presented to the south of 39°N and low eddy variability to the area north of 40°N and 41°N, bordering the Polar Front of the East Sea. The SSHA snapshots of the longest track in the Fig. 1 reveal the spatial features of the eddy variability in the East Sea as shown in Fig. 5, though the eddy patterns of each snapshot are somewhat different. The snapshot starts from about 35°N and directs northeast up to

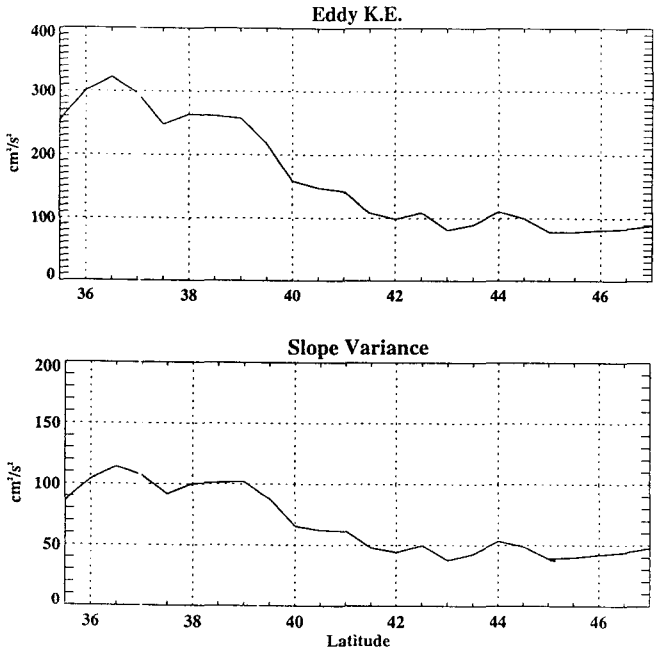

Fig. 4. Zonally averaged eddy kinetic energy (top) and slope variance (bottom) in the East Sea from five-year Topex/Poseidon altimeter data.

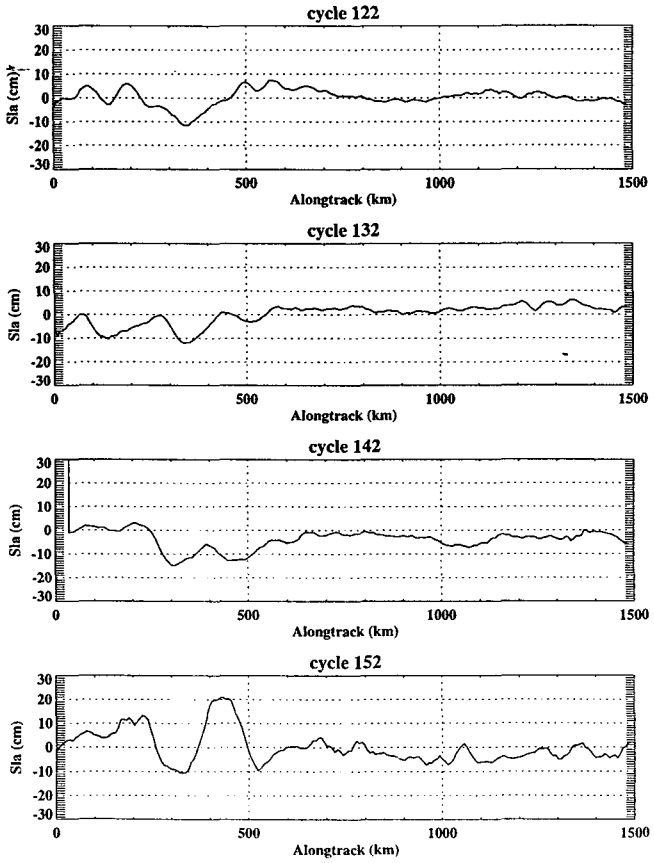

Fig. 5. Snapshots of sea surface height anomaly in the longest subtrack (Fig. 1). The snapshots are an interval of 10 cycles and measured on January (Cycle 122), April (Cycle 132), July (Cycle 142), and October (Cycle 152) of 1996.

northeastern end of the East Sea with very fast speed (about 4 min.). The snapshots are an interval of 10 cycles and measured on January (Cycle 122), April (Cycle 132), July (Cycle 142), and October (Cycle 152) of 1996, respectively. The high variability is quite common feature in the south and the relatively calm in the north. In the snapshots, we can deduce that the mesoscale eddies seem to be active in the southern area from the different pattern in different observation time. The snapshot in cycle 152 shows relatively high variability over the whole track compared to others. The high eddy variability in the south of the East Sea in the present study is consistent with that of the major surface current system such as Kuroshio, Gulf Stream, California Current, etc. (Richardson, 1983; Zlontnicki, 1989; Stammer, 1997) and that of previous studies in the East Sea (Toba et al., 1984; Isoda and Saitoh,

1993; Isoda, 1994; Lie et al., 1995; Shin et al., 1995; Jacobs et al., 1999).

The monthly mean variation of the surface EKE in the East Sea is computed from the five-year Topex/Poseidon measurements. Fig. 6 shows five-year monthly mean EKE averaged over the whole East Sea. The monthly EKE, standard deviation, and the number of data used in the calculation of the EKE are presented in Table 1. Because of the instability of the Topex/Poseidon spacecraft in the initial stage, the first seven cycles which cover mainly the period of October and November, 1992, are not used in the present study (Fu et al., 1994). The removal of the first seven cycles is reflected as small valid number of data in October and November of Table 1. The monthly mean sequence of EKE has a very simple structure, showing high variability in the period from October to February and a relatively low variability from March to September. The standard deviation of the monthly mean EKE is quite large compared to the mean EKE (Table 1), which suggests that the spatial variability of EKE in the East Sea is considerable for all months. To compare the monthly sequence of the EKE with wind stress curl, which is one of eddy generating mechanism, the monthly mean wind stress curl over the East Sea is generated from daily European Centre for Medium-Range Weather Forecasts (ECMWF) analysis for the corresponding period (October 1992 through September 1997) of the Topex/Poseidon altimeter data used in the present study (Fig. 7). The monthly sequences of the wind stress curl and EKE averaged over the whole East Sea show a resemblance (correlation coefficient 0.82). Thus it is hypothesized that the monthly variation of the EKE is forced by a monthly variation of wind stress curl in the East Sea. The high EKE in October seems to be related with the seasonality of the Tsushima Warm Current which expands its strength during summer and fall seasons. The weak peak in June is not clear in the present study.

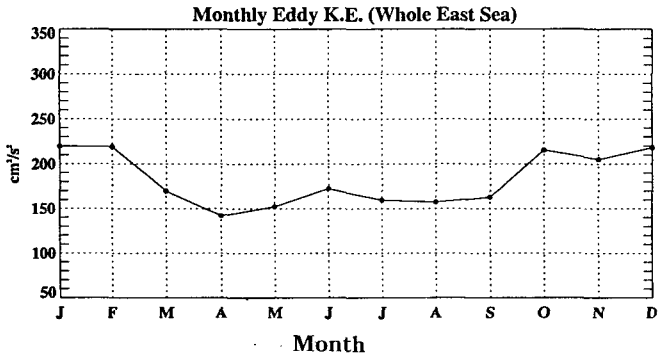

Fig. 6. Monthly eddy kinetic energy averaged for the whole East Sea from the five-year Topex/Poseidon altimeter data.

Table 1. Monthly mean eddy kinetic energy (EKE), standard deviation (SD), and the number of the data from the five-year Topex /Poseidon altimeter measurements

Month	EKE	SD	No. of Data
Jan.	219.89	322.63	12,789
Feb.	219.35	346.13	12,540
Mar.	169.90	238.93	13,397
Apr.	141.98	204.21	12,644
May	152.37	227.61	12,402
Jun.	172.59	281.78	12,031
Jul.	159.70	250.92	13,017
Aug.	157.46	237.77	12,101
Sep.	162.91	265.95	12,704
Oct.	215.44	392.31	10,653
Nov.	205.10	310.17	11,244
Dec.	218.38	325.43	13,189

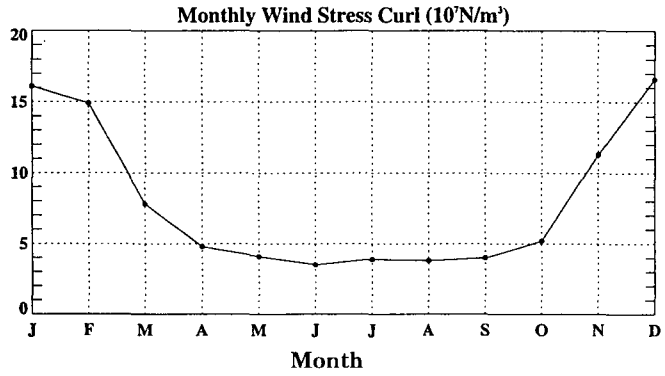

Fig. 7. Monthly mean wind stress curl averaged for the whole East Sea from the five-year (October 92~September 97) ECMWF daily wind stress data.

In order to describe the regional characteristics of the monthly mean EKE in the East Sea, the monthly mean EKE time series are separated into three regions with low, medium, and large eddy activities as Fig. 3 and plotted in Fig. 8. Due to the spatial difference in the amplitude of eddy variability, the different EKE's scales are used in Fig. 8. The regional monthly time series of eddy variability show quite similar pattern to the overall monthly time series in Fig. 6, especially in the low and medium

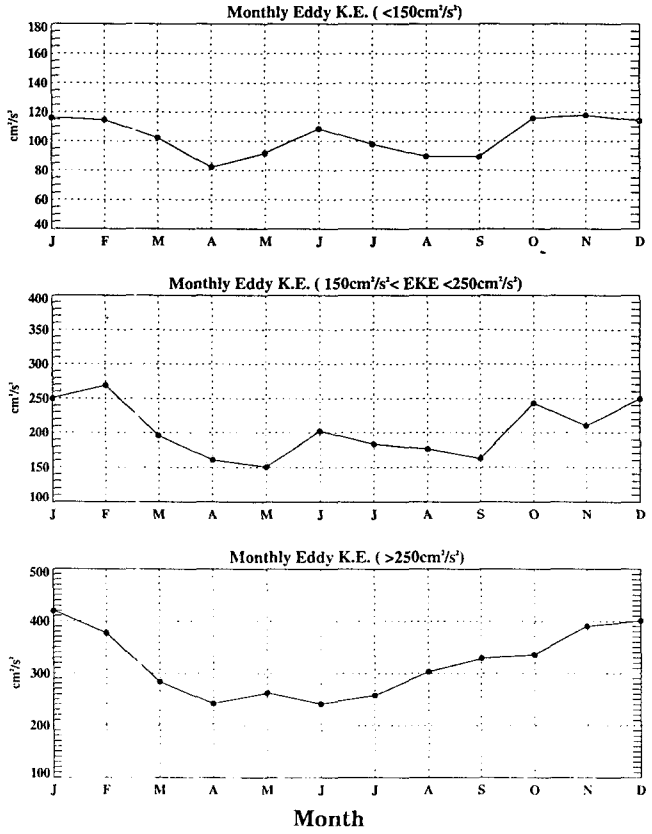

Fig. 8. Monthly eddy kinetic energy averaged for the low (top panel), medium (middle panel), and high (bottom panel) energy areas classified as Fig. 3 in the East Sea from the five-year Topex/Poseidon altimeter data.

eddy areas. In general, the eddy variability is high in fall and winter in spite of the background EKE difference. In low variability area, the relative peak in eddy energy is presented in October through February as shown in the top panel of Fig. 8. The EKE in the low area is quite small from April to September except June as in Fig. 6. The moderate peak EKE of the low variability area in June is not clear in the present study. In the area of medium variability (middle panel of Fig. 8), the monthly pattern of EKE is quite similar to that of low variability time series as shown in top panel of Fig. 8. In the area of high variability (bottom panel of Fig. 8), the monthly EKE time series show a distinct characteristic in addition to the common seasonal pattern such that the EKE shows its steady increase from August. The increase of EKE from August in the high variability area is believed to be related with the seasonality of the Tsushima Warm Current which shows its maximum strength during summer and fall seasons.

In order to find the seasonal variability and to check possible correlation with wind forcing, the seasonal mean variation of the surface EKE is calculated with the five-year Topex/Poseidon measurements. The seasons are divided into spring (S) from April to June, summer (S) from July to September, fall (F) from October to December, and winter (W) January to March, respectively. The seasonal division is followed by Zlontnicki et al. (1989) for the comparison with their study. The seasonal sequence of the EKE averaged over the whole East Sea is shown in Fig. 9. As shown in monthly map (Fig. 6 and Fig. 8), the seasonal EKE shows a trend repeating high EKE in the fall and winter (October ~March) and low EKE in spring and summer (April~September). This result is consistent with the sea level variance pattern in the northeastern Pacific Ocean from Geosat altimeter data (Zlontnicki et al., 1989). The interannual variability of the seasonal EKE is shown but the amplitude is not large. Fig. 10 shows a corresponding seasonal sequence of wind stress curl averaged over the whole East Sea based on ECMWF wind stress data. The sequential pattern of wind stress curl over the East Sea also shows a resemblance with that of seasonal EKE. Two sequences (Fig. 9 and Fig. 10) have a correlation coeficient of 0.67, providing an evidence that wind stress curl is a possible forcing for the seasonal variation of the EKE in the East Sea as

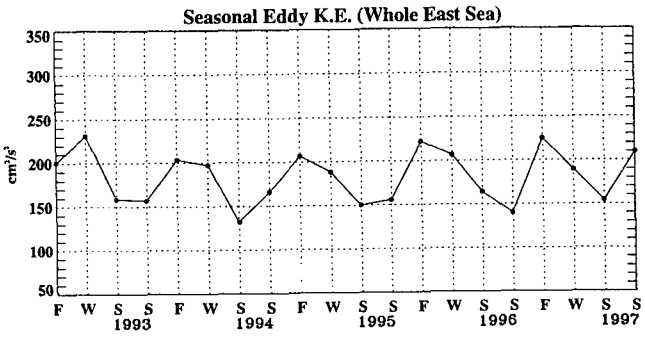

Fig. 9. Seasonal eddy kinetic energy averaged for the whole East Sea from the five-year Topex/Poseidon altimeter data. The seasons are divided into spring (S) from April to June, summer (S) from July to September, fall (F) from October to December, and winter (W) January to March, respectively.

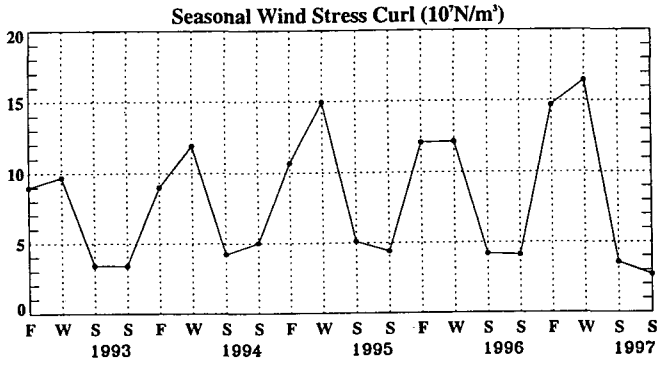

Fig. 10. Seasonal mean wind stress curl averaged for the whole East Sea from the five-year ECMWF daily wind stress data. The seasons are divided into spring (S) from April to June, summer (S) from July to September, fall (F) from October to December, and winter (W) January to March, respectively.

shown in the monthly sequences. However, the peak EKE appears in the fall generally but the peak wind stress curl does in the winter. This feature can be explained from the seasonality of the Tsushima Warm Current which shows its maximum strength during summer and fall seasons as explained above. As monthly time series of EKE (Fig. 8), the seasonal mean sequences of EKE in the East Sea are separated into three regions of low, medium, and high eddy activities and then presented in Fig. 11. In general, the regional pattern of seasonal EKE (Fig. 11) is similar to the whole pattern of seasonal EKE averaged for whole East Sea (Fig. 9). However, the interannual variability of the regional EKE is also superposed into the seasonal sequences in addition to the regular pattern shown in Fig. 9. The correlation coefficients between each seasonal sequence of the EKE (Fig. 11) and wind stress curl (Fig. 10) are 0.70, 0.60, and 0.71, respectively. The medium eddy area mainly located in the transition and eddy propagation route of the East Sea shows relatively lower correlation with wind stress curl than other areas.

Summary

We have described the eddy variability in terms of sea surface height anomaly, slope variability, and eddy kinetic energy based on the five-year (October 1992~September 1997) Topex/Poseidon altimeter

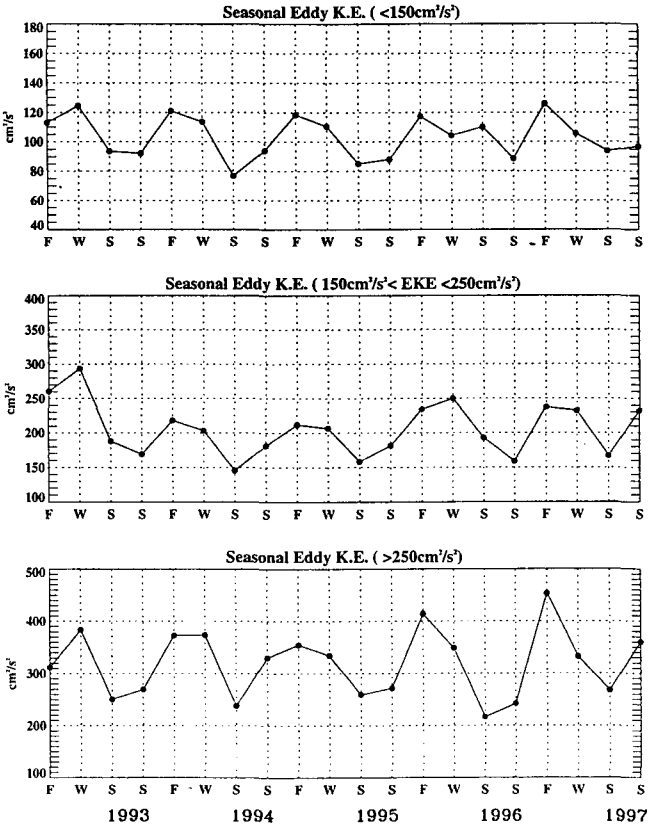

Fig. 11. Seasonal eddy kinetic energy averaged for the low (top panel), medium (middle panel), and high (bottom panel) energy areas classified as Fig. 3 in the East Sea from the five-year Topex/Poseidon altimeter data. The seasons are divided into spring (S) from April to June, summer (S) from July to September, fall (F) from October to December, and winter (W) January to March, respectively.

measurements over the East Sea. The eddy variability in the East Sea is mainly described with eddy kinetic energy in the present study. The method calculating surface eddy kinetic energy is based on the assumption of a geostrophic relation and isotropic condition of the mesoscale eddy in the East Sea. This method has been shown by Stammer (1997) to be consistent with the EKE from thermal wind method with hydrographic observations for the global application and by Kelly et al. (1998) from drifter data for the California Current.

We find that there exists a distinct spatial contrast of the eddy variability in the East Sea such that high eddy energy distributed in the south and low eddy energy in the north, bordering the Polar

Front of the East Sea based on the five-year Topex /Poseidon altimeter data. The high eddy variability in the south of the East Sea is closely connected with the paths of the Tsushima Warm Current which governs the surface flow system in the south of the East Sea. This fact suggests that the high eddy variability in the south of the East Sea is generated by the baroclinic instability process due to the Tsushima Warm Current. This result is consistent with previous studies in the East Sea (Toba et al., 1984; Isoda and Saitoh, 1993; Isoda, 1994; Lie et al., 1995; Shin et al., 1995; Jacobs et al., 1999) and other oceans (Zlontnicki et al., 1988; Stammer, 1997; Strub et al, 1997; Kelly et al., 1998, etc) which have shown the strong eddy energy coupled with major current system. The EKE is relatively low in the north of the Polar Front except in the region north of 39°N and west of 133°E (Fig. 3), where the eddies appear frequently. The monthly variation and seasonal sequence of the EKE show a strong seasonality in both areas of high and low eddy variability such as a high EKE from October to February and a relatively low EKE from March to September. The sequential pattern of wind stress curl shows a resemblance with that of seasonal EKE and the two sequences have a correlation coefficient of 0.67, providing an evidence that wind stress curl is a possible forcing for the seasonal variation of the EKE in the East Sea. The seasonality of the EKE also seems to correlate with the seasonality of the Tsushima Warm Current, especially in the area of high eddy variability. There also exists a large spatial variability and interannual variability in the eddy variability in the East Sea.

In this study we tried to describe the eddy variability in the East Sea with statistical approach rather than dynamical one. One of the limitation in the present study is the assumption of isotropic condition in calculating EKE because of the spatial sampling interval of the Topex/Poseidon altimeter. The isotropic assumption is successfully applied to the eddy variability for the large-scale open ocean such as Stammer (1997). In the regional study such as California Current (Strub et al., 1997), the polarization of eddy variability is quite a common feature, especially in the areas bounded by land. In this respect, the eddy variability in the East Sea can be biased with the variability from the data with a high spatial resolution. It is recommended that the Topex/Poseidon data be combined with the ERS (European Remote Sensing) data with a higher crosstrack resolution, the Jason data complementing the low crossspatial sampling of the Topex/Poseidon and be compared with observation data such as drifter data and direct current measurements. Also the calculation of geostrophic current using satellite alongtrack data is a kind of high-pass filter in which the noise of altimeter measurements can be contained. We used the low-pass filter with a half-amplitude distance of about 40 km based on Strub et al. (1997) and Kelly et al. (1998). However, the signal to noise can be different depending on the ocean applied and thus further study is required to recover the true signal of the current from altimeter data by comparing with direct observation such as drifters and current meter observations. Also spatial distribution of the eddy variability is quite limited in the present study because of the poor sampling in the cross-track direction of the Topex/Poseidon mission. The limitation would be improved with use of the ERS and Jason data.

Acknowledgement

The authors express their gratitude to the two anonymous reviewers for their critical and constructive comments and suggestions. The Topex/Poseidon altimeter data are supplied by the CLS Space Oceanographic Division, Toulouse, France and the NASA Physical Oceanography Distributed Active Archive Center at the Jet Propulsion Laboratory/ California Institute of Technology, USA. The work was supported by the Korea Research Foundation Grant (KRF-1997-037-H00119).

References

AVISO. 1997. AVISO-Handbook Sea Level Anomalies AVI-NT-011-312-CN, Edition 3.0, CLS, France, 24pp.

Cartwright, D.E. and R.J. Tayler. 1971. New computations of the tide-generating potential. Geophys. J. R. Astr. Soc., 33, 253~264.

Chelton, D.B. 1988. WOCE/NASA altimeter Algorithm Workshop, U.S. WOCE Technical Report Number 2, U.S. Planning Office for WOCE, College Station, TX, USA, 70 pp.

Eanes, R.J. and S.V. Bettadpur. 1995. The CSR 3.0 global

ocean tide model. CSR-TM-95-06. Center for Space research, Univ. of Texas at Austin.

Fu, L.-L., E.J. Christensen, C.A. Yamarone, M. Lefebvre, Y. Menard, M. Dorrer and P. Escudier. 1994. Topex/Poseidon mission overview. J. Geophys. Res., 99, 24369~24382.

Fu, L.-L. and R.A. Davidson. 1995. A note on the barotropic response of sea level to time-dependent wind forcing. J. Geophys. Res., 100, 24955~24964.

Fu, L.-L. and V. Zlontnicki. 1989. Observing ocean mesoscale eddies from Geosat altimetry: Preliminary results. Geophys. Res. Lett., 16, 457~460.

Gasper, P. and F. Ogor. 1996. Estimation and analysis of the sea state bias of the new ERS-1 and ERS-2 altimetric data. Technical Report. IFREMER/CLS.

Isoda, Y. 1994. Warm eddy movements in the eastern Japan Sea. J. Oceanogr., 50, 1~15.

Isoda, Y. and S.I. Saitoh. 1993. The northward intruding eddy along the east coast of Korea. J. Oceanogr., 49, 443~458.

Jacobs, G.A., P.J. Hogan and K.R. Whitmer. 1999. Effects of eddy variability on the circulation of the Japan/East Sea. J. Oceanogr., 55, 247~256.

Lie, H.J., S.K. Byun, I. Bang and C.H. Cho. 1995. Physical structure of eddies in the southwestern East Sea. J. Korean Soc. Oceanogr., 30, 170~183.

Kelly, K.A., R.C. Beardsley, R. Limeburner and K.H. Brink. 1998. Variability of the near-surface eddy kinetic energy in the California Current based on altimetric, drifter, and moored current meter. J. Geophys. Res., 103, 13067~13083.

McWilliams, J.C. 1983. The local dynamics of eddies in the western North Atlantic: Eddies in Marine Science. Springer-Verlag, 609pp.

Muller, P. and C. Frankignoul. 1981. Direct atmospheric forcing of geostrophic eddies. J. Phys. Oceanogr., 11, 287~308.

PO.DAAC. 1997. Merged GDR B (Topex/Poseidon) User's Handbook, JPL, USA, 124pp.

Richardson, P.L. 1983. Eddy kinetic energy in the North Atlantic from surface drifters. J. Geophys. Res., 88, 4355~4367.

Richman, J.G., C. Wunsch and N.G. Hogg. 1977. Space and time scales and mesoscale motion in the sea. Rev. Geophys., 15, 385~420.

Robinson, A.R. 1993. Eddies in Marine Science. Springer-Verlag, 609pp.

Shin, H.R., S.K. Byun, C. Dim, S. Hwang and C.W. Shin. 1995. The characteristics of structure of warm eddy observed to the northwest of Ullung in 1992. J. Korean Soc. Oceanogr., 30, 39~56.

Stammer, D. 1997. Global characteristics of ocean variability estimated from regional Topex/Poseidon altimeter measurements. J. Phys. Oceanogr., 27, 1743~1769.

Stammer, D. and C. Wunsch. 1994. Preliminary assessment of the accuracy and precision of Topex/Poseidon altimeter data with respect to the large-scale ocean circulation. J. Geophys. Res., 99, 24584~24604.

Strub, P.T., T.K. Chereskin, P.P. Niiler, C. James and M.D. Levine. 1997. Altimeter-derived variability of surface velocities in the California Current System, 1, Evaluation of Topex altimeter velocity resolution. J. Geophys. Res., 102, 12727~12748.

Toba, Y., H. Kawamura, F. Yamashita and K. Hanawa. 1984. Structure of horizontal turbulence in the Japan Sea. pp. 317~332. In Ocean Hydrodynamics of the Japan and East China Seas, ed. by T. Ichiye, Elsevier, Amsterdam.

Treguier, A.M. and B.L Hua. 1988. Influence of bottom topography on stratified quasi-geostrophic turbulence in the ocean. J. Astrophys. Fluid Dyn., 43, 265~305.

Wunsch, C. and D. Stammer. 1995. The global frequency-wavenumber spectrum of oceanic variability estimated from Topex/Poseidon altimeter measurements. J. Geophys. Res., 100, 24895~24910.

Wyrti, K., L. Magaard and J. Hager. 1976. Eddy energy in the oceans. J. Geophys. Res., 81, 2641~2646.

Zlontnicki, V., L.-L. Fu and W. Patzert. 1989. Seasonal variability in global sea level observed with Geosat altimetry. J. Geophys. Res., 94, 17959~17969.